Biogeosciences
Discussions

Open Access

Spatial variations in the Kuroshio nutrient transport from the East China Sea to south of Japan

X. Y. Guo[1,2], X.-H. Zhu[1,3], Y. Long[1], and D. J. Huang[1,3]

[1]State Key Laboratory of Satellite Ocean Environment Dynamics, Second Institute of Oceanography, State Oceanic Administration Hangzhou, 310012, China
[2]Center for Marine Environmental Study, Ehime University, 2–5 Bunkyo-cho, Matsuyama 790-8577, Japan
[3]Department of Ocean Science and Engineering, Zhejiang University, Hangzhou, 310058, China

Discussion Paper | Discussion Paper | Discussion Paper | Discussion Paper |

BGD

10, 6737–6762, 2013

Kuroshio nutrient transport from the East China Sea to south of Japan

X. Y. Guo et al.

Title Page

Abstract | Introduction

Conclusions | References

Tables | Figures

◄◄ | ►►

◄ | ►

Back | Close

Full Screen / Esc

Printer-friendly Version

Interactive Discussion

Abstract

Based on absolute geostrophic velocity calculated from repeated hydrographic data of 39 cruises from 2000 to 2009 and nitrate concentrations measured at the same sections from 1964 to 2011, we obtained temporally averaged nitrate flux (the product of velocity and nitrate concentration) and nitrate transport (integration of flux over a section) through 4 sections along the Kuroshio path from the East China Sea (sections PN and TK) to south of Japan (sections ASUKA and 137E). In addition, we examined section OK east of the Ryukyu Islands in order to understand the contribution of Ryukyu Current to the Kuroshio nutrient transport south of Japan. The mean nitrate flux shows a subsurface maximum core with a value of 10, 10, 11, 11, and 6 mol m^{-2} s^{-1} at sections PN, TK, ASUKA, 137E, and OK, respectively. The depth of subsurface maximum core changes among five sections and is approximately 400, 500, 500, 400, and 800 m at sections PN, TK, ASUKA, 137E, and OK respectively. The mean downstream nitrate transport is 199.3, 176.3, 909.2, 1385.5, and 341.2 kmol m^{-1} at sections PN, TK, ASUKA, 137E, and OK respectively. The nutrient transports at these sections suggest the presence of Kuroshio nutrient stream from its upstream region to downstream. The deep current structure of Ryukyu Current (section OK) makes it contribute more nitrate transport than the Kuroshio in the East China Sea (section TK) to the Kuroshio south of Japan. In addition, the positive difference between the downstream nitrate transport through section ASUKA and the sum of nitrate transports through sections TK and OK, as well as the positive difference of downstream nitrate transport between sections 137E and ASUKA, suggest that the Kuroshio recirculation significantly intensifies the downstream (eastward) nitrate transport by the Kuroshio.

1 Introduction

Strong western boundary current carries huge amount of water mass and heat as well as a variety of dissolved materials including nutrients, and has a significant influence

on climate and marine ecosystem around its path. Pelegrí and Csanady (1991) and Pelegrí et al. (1996) reported a subsurface maximum in the nutrients flux (the product of velocity and nutrients concentration) in the Gulf Stream, and first proposed the presence of nutrient stream, a continuous nutrient transport, along the Gulf Stream from its
5 upstream to downstream.

As a result of reduced current speed and increased nutrient concentration with depth, the nutrient flux has a subsurface high value (Pelegrí and Csanady, 1991). Chen et al. (1994, 1995) calculated the Kuroshio nutrient flux based on four cruises along a section east of Taiwan, and reported the presence of subsurface maximum core of
10 nutrient flux at 500 m depth. Guo et al. (2012) obtained a long-term averaged nutrient flux at section PN (see Fig. 1b for its location) based on situ data from 88 cruises from 1987 to 2009 and demonstrated a subsurface maximum core of nutrient flux at 400 m depth in the long-term averaged nutrient flux. Comparing the nutrient fluxes at section east of Taiwan and at section PN, the depth of subsurface maximum core of nutrient
15 flux likely changes along the pathway of the Kuroshio. However, except for these two sections, we know little on the vertical structure of nutrient flux along the Kuroshio path from the East China Sea to south of Japan.

Guo et al. (2012) reported a value of 170.8 kmol s^{-1} as a long-term averaged nitrate transport (integration of flux over a section) of the Kuroshio at section PN in the East
20 China Sea. This is the only value we know on the nutrient transport by the Kuroshio. Therefore, we still have no answer on the presence of Kuroshio nutrient stream from its upstream to downstream.

In this paper, we calculated nitrate flux and nitrate transport through 4 sections along the Kuroshio path from the East China Sea (sections PN and TK) to south of Japan
25 (sections ASUKA and 137E). In addition, we also examined section OK east of the Ryukyu Islands where the Ryukyu Current flows (Zhu et al., 2004). By examining nutrient flux and nutrient transport at five sections, we want to confirm the presence of Kuroshio nutrient stream from the East China Sea to south of Japan, reveals the spatial

variations of Kuroshio nutrient flux and nutrient transport along the Kuroshio path, and clarify the factors controlling the spatial variations in the Kuroshio nutrient transport.

2 Data and analysis method

The hydrographic data from winter 2000 to fall 2009 and nutrient data from 1964 to 2011 at sections PN, TK, ASUKA, 137E and OK (Fig. 1b) were obtained from Japan Meteorological Agency (JMA, http://www.data.kishou.go.jp/kaiyou/db/vessel_obs/data-report/html/ship/ship.php). The hydrographic data were collected by CTD (Conductivity Temperature Depth profiler); the nutrient data were from water samples collected at standard depths and analyzed using routine methods (see Table 1 in Aoyama et al. (2008) for analysis method details). Figure 2 summarizes the availability of hydrographic and nutrient data at five sections.

Hydrographic data at sections PN, TK, ASUKA, 137E and OK from winter 2000 to fall 2009 (Fig. 2) were used in the inverse calculation for the absolute geostrophic velocity. Since the inverse calculation needs CTD data at all the sections, we limited to the period from winter 2000 to fall 2009 when this condition is approximately satisfied. The inverse method (Wunsch, 1978) was applied to the 3 areas enclosed by 5 sections, the line connecting two stations at north end of sections PN and TK, and the coastline of southern Japan (Fig. 1b). The water exchange through two gaps between the islands at the southwestward extension of section TK was neglected. The water column was vertically separated into eight layers bounded by the sea surface and 8 isopycnals (24.80, 25.50, 26.50, 27.00, 27.30, 27.50, 27.60, $27.66\sigma_\theta$). Mass conservation was assumed within each of 8 layers, while salt conservation was assumed within the lower 7 layers. With these conditions, the velocities at the reference level, which was set as the depth of deepest hydrographic data between each pair of stations or sea bottom, were obtained (Zhu et al., 2006). Applying the thermal winds relation to a pair of hydrographic stations, we obtained the absolute geostrophic velocity normal to the line connecting two stations at one meter interval in the vertical direction. We denote

the absolute geostrophic velocity at one section as $V(x, z, t)$, where x is horizontal distance from left side of the section, z is water depth, t is time of cruise. As shown in Fig. 2, we can find hydrographic data at the same season for all the five section in most cases. In the case there was no hydrographic data at the same season for all the five sections, we used mean hydrographic field at the same season at the section without hydrographic data. Such case occurred mostly at section OK (Fig. 2).

To calculate nutrient flux, we need nutrient concentration at grid point of velocity. The nutrients in the JMA dataset have nitrate and phosphate concentrations but not silicate. Since nitrate and phosphate concentrations have a good linear correlation (Guo et al., 2012), we focus on nitrate in this study. The nitrate concentrations at standard levels were first linearly interpolated to depth at one meter interval at the hydrographic stations along a section and then were linearly interpolated horizontally to the grid point of velocity at the same depth, which were defined at the middle of two hydrographical stations. We denote nitrate concentration at a section as $C(x, z, t)$. The nutrient flux, $F(x, z, t)$, defined as product of velocity and nutrient concentration, was calculated by $F(x, z, t) = V(x, z, t)C(x, z, t)$.

Our purpose is to know the mean value of nutrient flux by the Kuroshio from all the cruises at a section. A common way to obtain such mean value is the direct average of nutrient flux from each cruise as shown in following equations,

$$F_0(x, z) = \frac{1}{N} \sum_{k=1}^{N} F(x, z, t_k) = \frac{1}{N} \sum_{k=1}^{N} V(x, z, t_k)C(x, z, t_k) \tag{1}$$

where, $F_0(x, z)$ is mean value of nutrient flux; subscript k is number for time index, N is total number of cruises. The calculation of $F(x, z, t_k)$ needs both current speed and nutrient concentration from the same cruise. However, nitrate concentration was not sampled for section TK from winter 2000 to fall 2009, and was not sufficiently sampled for section ASUKA from winter 2000 to fall 2009 (Fig. 2). Therefore, it is difficult to use Eq. (1) to calculate $F(x, z, t_k)$ for all the cruises from winter 2000 to fall 2009 at these two sections. Instead, we temporally averaged nitrate concentrations at two sections

Full Screen / Esc

Printer-friendly Version

Interactive Discussion

from all the cruises that reported nitrate concentration by following equation,

$$C_0(x,z) = \frac{1}{N_0} \sum_{k=1}^{N_0} C(x,z,t_k) \tag{2}$$

where, $C_0(x,z)$ is mean nitrate concentration, N_0 is total number of cruises for nitrate data at sections TK or ASUKA. Then, we used $C_0(x,z)$ to replace $C(x,z,t_k)$ in Eq. (1)

5 and obtained $F(x,z,t_k)$ for all the cruises from winter 2000 to fall 2009 at two sections.

This replacement actually introduces an error in mean nitrate flux $F_0(x,z)$. The nutrient concentration at a fixed place from a cruise $C(x,z,t)$ contains a mean component $C_0(x,z)$ and its temporally varying component $C'(x,z,t)$, i.e. $C(x,z,t) = C_0(x,z) + C'(x,z,t)$. Similarly, the current speed at a fixed place from a cruise $V(x,z,t)$ has

10 also a mean component $V_0(x,z)$ and a temporally varying component $V'(x,z,t)$, i.e. $V(x,z,t) = V_0(x,z) + V'(x,z,t)$ and $V_0(x,z) = \frac{1}{N} \sum_{k=1}^{N} V(x,z,t_k)$. With such separation, the mean nutrient flux becomes,

$$F_0(x,z) = V_0(x,z)C_0(x,z) + \frac{1}{N} \sum_{k=1}^{N} V'(x,z,t_k)C'(x,z,t_k). \tag{3}$$

According to Eq. (3), the mean nutrient flux at a fixed point composes of two compo-

15 nents. One is the product of mean current speed and mean nutrient concentration. The other is the temporal average of product of temporally varying components of current speed and nutrient concentration. Apparently, the calculations of $F_0(x,z)$ at sections TK and ASUKA neglects the contribution of second term in r.h.s of Eq. (3). This is first problem in the calculation of mean nutrient flux at sections TK and ASUKA. The sec-

20 ond problem is the difference between the mean nutrient concentration calculated by Eq. (2) and the unknown mean nutrient concentration from winter 2000 to fall 2009. As discussed in Sect. 4, these two problems are not serious to our conclusions.

The spatial integral of $F_0(x,z)$ in a given area becomes nutrient transport through the area. In order to avoid pseudo spatial variation of nutrient transport along a section due to different horizontal distance of hydrographic stations, we resampled $C_0(x,z)$, $V_0(x,z)$, $F_0(x,z)$ by dividing a section using an unit width of 25 km in the horizontal direction and 1 m interval in the vertical direction. We denote resampled variables as $C_0(i,j)$, $V_0(i,j)$, $F_0(i,j)$, where i and j are indexes in horizontal and vertical directions, respectively. Based on the resampled variables, we obtained three variables at each of eight isopycnal layers (l) for each section, i.e. spatially averaged nitrate concentration within unit width $C_0(i,l)$, volume transport per unit width $VT_0(i,l)$, and nitrate transport per unit width $NT_0(i,l)$, by following equations.

$$C_0(i,l) = \frac{1}{j_2 - j_1 + 1} \sum_{j=j_1}^{j_2} C_0(i,j) \tag{4}$$

$$VT_0(i,l) = \sum_{j=j_1}^{j_2} V_0(i,j)\Delta x \tag{5}$$

$$NT_0(i,l) = \sum_{j=j_1}^{j_2} F_0(i,j)\Delta x \tag{6}$$

where, l is index for 8 isopycnal layers, j_1 and j_2 are two depth indexes for upper end and lower end of one isopycnal layer, Δx is unit width (25 km). The vertical sum of $VT_0(i,l)$ and $NT_0(i,l)$ for $l = 1,8$ produces the volume transport $VT(i)$ and nutrient transport $NT(i)$ within unit width along a section. The horizontal sum of $VT_0(i,l)$ and $NT_0(i,l)$ for $i = 1,M$ (M is grid number of a section in horizontal direction) produces total volume transport $VT(l)$ and nutrient transport $NT(l)$ in one isopycnal layer of a section; the horizontal sum of $VT(i)$ and $NT(i)$ for $i = 1,M$ or the vertical sum of $VT(l)$ and $NT(l)$ for $l = 1,8$ produces total volume transport VT and total nutrient transport NT through a section.

As presented in Sect. 3, the recirculation south of the Kuroshio is very important to the eastward nutrient transport by the Kuroshio south of Japan. To know the contribution of recirculation, we defined positive values for nutrient flux and nutrient transport at a section if they have the same direction (approximately eastward) as the Kuroshio or Ryukyu Current; negative values for nutrient flux and nutrient transport if they have an opposite direction (approximately westward) as the Kuroshio or Ryukyu Current. We use superscript "+" ("−") to represent positive (negative) velocity, nutrient flux and nutrient transport.

3 Results

3.1 The current fields at five sections

The temporally averaged velocity present a consistent picture for the Kuroshio from the East China Sea (Fig. 3a, b) to south of Japan (Fig. 3c, e). In the East China Sea, the surface current speed exceeds $1\,\mathrm{m\,s^{-1}}$ above the shelf break at section PN and exhibits a structure with a single maximum speed core around 28.3° N. The current reduces its speed in proportion to the distance from the maximum speed core in both horizontal and vertical directions. The current speed exceeds $0.1\,\mathrm{m\,s^{-1}}$ at 600 m depth, showing a high potential for carry dissolved material to its downstream in the subsurface layer.

At the Tokara Strait, the exit of Kuroshio from the East China Sea, the current shows two maximum speed cores at southern and northern channels, respectively (Fig. 3b). The surface maximum current speed at the Tokara Strait is lower at southern channel than at northern channel and both of them are lower than that at section PN. Although the surface current is weaker at the Tokara Strait than at section PN, the weakening of current speed with depth is also weaker in the Tokara Strait than at section PN. Consequently, the current speed is kept as $0.3\,\mathrm{m\,s^{-1}}$ at 600 m depth in the southern channel of Tokara Strait.

At section ASUKA (Fig. 3c), the Kuroshio is significantly intensified, which may be understood by the large area with a current speed larger than $0.9\,\mathrm{m\,s^{-1}}$ and the offshore extension of area with a current speed larger than $0.1\,\mathrm{m\,s^{-1}}$. The eastward volume transport at section ASUKA is 62.6 Sv, which is much larger than those at section PN (26.8 Sv) and section TK (23.5 Sv) (Table 1). On the other hand, an opposite current south of the Kuroshio is easily identified. The speed of this counter current is much weaker than the Kuroshio but its presence is identified over a larger region.

The current structure at section 137E (Fig. 3e) is similar with that at section ASUKA, i.e. a strong and robust eastward Kuroshio and a weak but wide westward counter current. A different point is the distance of the Kuroshio from the coastline. The Kuroshio flows farther away from the coastline at section 137E than at section ASUKA. A counter current appears at inshore side of the Kuroshio at section 137E (Fig. 3e).

The current is weak in the surface layer but strong in the subsurface at section OK (Fig. 3d). This is a well-known feature of Ryukyu Current (Zhu et al., 2004), a branch current of the Kuroshio in the East China Sea (Andres et al., 2008). Although it is not very clear in Fig. 3d, a maximum speed core can be identified at 600 m depth. The eastward volume transport is 16.4 Sv at section OK.

The eastward volume transport is 26.8 Sv at section PN and 23.5 Sv at section TK, changing little in the East China Sea. The combination of eastward volume transport at sections TK and OK is ~ 40.0 Sv, being less than that (62.6 Sv) at section ASUKA. Although sections ASUKA and 137E are both at south of Japan and not far away from each other, the eastward volume transport increase by 13.5 Sv from section ASUKA to section 137E (76.1 Sv, Table 1).

The increasing of eastward volume transport of the Kuroshio south of Japan is caused by the counter current south of the Kuroshio, i.e. Kuroshio recirculation. The eastward volume transport of the Kuroshio south of Japan consists of two parts: one from itself that is related to basin-scale wind stresses while the other from the anticyclonic recirculation gyre, a local current system south of the Kuroshio (Hasunuma and Yoshida 1978). Imawaki et al. (2001) indicated a significant contribution

Kuroshio nutrient transport from the East China Sea to south of Japan

X. Y. Guo et al.

Full Screen / Esc

Printer-friendly Version

Interactive Discussion

of recirculation to the eastward volume transport of the Kuroshio measured at section ASUKA. Ichikawa et al. (2004) also noted its influences on the Ryukyu Current and attributed an increasing in volume transport from section OK (Zhu et al., 2004) to a section southeast of Amami island to the presence of Kuroshio recirculation.

3.2 Nitrate concentrations and nitrate fluxes at five sections

The temporally averaged nitrate concentration has relatively simple distribution at 5 sections (Fig. 3). In general, the nitrate concentration increases with depth: approximately zero at sea surface, $5 \, \mathrm{mmol \, m^{-3}}$ around 100–200 m depth, $35 \, \mathrm{mmol \, m^{-3}}$ around 700–800 m depth, and $\sim 40 \, \mathrm{mmol \, m^{-3}}$ below 1000 m depth. The vertical varying rate of nitrate concentration is small in the surface layer (0–200 m), large in the subsurface layer (200–1000 m), and small again in the deep layer (> 1000 m). The horizontal variations in mean nitrate concentration at these sections are found only near the shelf slope where the contour lines of nitrate concentration raise toward the shallow shelf region (Fig. 3).

The temporally averaged nitrate flux has a consistent subsurface maximum core at 5 sections (Fig. 4). The depth of subsurface maximum core is relative stable along the Kuroshio path: 400 m at section PN, 500 m at section TK, 500 m at section ASUKA, and 400 m at section 137E. However, the corresponding isopycnal layer of subsurface maximum core changes a little along the Kuroshio path: $25.5–26.5\sigma_\theta$ at section PN, $\sim 26.5\sigma_\theta$ at section TK, $\sim 26.5\sigma_\theta$ at section ASUKA, $25.5–26.5\sigma_\theta$ at section 137E. The subsurface maximum core of nitrate flux at section OK is at depth of 800 m, corresponding to an isopycnal layer of $27.0\sigma_\theta$.

The nitrate flux at its subsurface maximum core is $10 \, \mathrm{mmol \, m^{-2} \, s^{-1}}$ at section PN, $10 \, \mathrm{mmol \, m^{-2} \, s^{-1}}$ at section TK, $11 \, \mathrm{mmol \, m^{-2} \, s^{-1}}$ at section ASUKA, $11 \, \mathrm{mmol \, m^{-2} \, s^{-1}}$ at section 137E, showing a stable value along the Kuroshio path. This value is $6 \, \mathrm{mmol \, m^{-2} \, s^{-1}}$ at section OK, being above half of it along the Kuroshio path. Since the current speed is weak at section OK, the high nitrate concentration at 800 depth is the direct reason for the good performance of Ryukyu Current in transporting nutrients

to south of Japan. In fact, the mean nitrate concentrations at the subsurface maximum core of nitrate flux are 17.5, 26.2, 25.2, 21.6, 36.0 mmol m^{-3} at sections PN, TK, ASUKA, 137E, OK, respectively, while the mean speeds at the subsurface maximum core of nitrate flux are 0.52, 0.40, 0.44, 0.51, 0.17 m s^{-1} at sections PN, TK, ASUKA, 137E, OK, respectively.

Since the maximum nitrate flux does not change largely along the Kuroshio, the nitrate transport through each section should be proportion to the area covered by the same contour of nitrate flux. Apparently, the area with the nitrate flux larger than 1 mmol m^{-2} s^{-1} significantly increases at sections ASUKA and 137E. Consequently, the eastward nitrate transports are higher at sections ASUKA and 137E than at sections PN, TK, and OK (Table 1).

Up to now, we mentioned only positive nitrate flux in Fig. 4. However, negative nitrate flux can be also found at all the sections (Fig. 4). This is in particular apparent for sections ASUKA and 137E, where an increasing of negative nitrate flux in the subsurface layer is observed for a wide region. This negative nitrate flux is caused by the weak but wide Kuroshio recirculation south of the Kuroshio (Fig. 4) and this westward nitrate transport also shows a downstream intensification with the Kuroshio (Table 1).

3.3 Horizontal distributions of nitrate transport through an unit width

In order to obtain a general image on horizontal distribution of nutrient transport in the study region, we present averaged nitrate concentration $C_0(i, l)$, volume transport $VT_0(i, l)$ and nitrate transport $NT_0(i, l)$ defined by Eqs. (4)–(6) for unit width within each of 8 isopycnal layers (Fig. 5). The eastward volume transport is large in the upper layers (Fig. 5a–c) but small in the lower layers (Fig. 5f–h). The counter current is apparent at sections ASUKA and 137E, located just south of the eastward Kuroshio (Fig. 5a–c). The nitrate concentration varies mainly in the vertical direction as known from the difference between the panels in the Fig. 5. The horizontal change in nitrate concentration among 5 sections in the same layer is little (Fig. 5).

The eastward nitrate transport can be confirmed in the 1st layer (Fig. 5a), becomes apparent for 2nd layer (24.8–25.5σ_θ) to 6th layer (27.3–27.5σ_θ), and is still large in two heaviest layers (Fig. 5g, h). An apparent intensification of eastward nitrate transport along the Kuroshio path from the East China Sea to south of Japan is evidenced from 2nd layer to 5th layer while that from section ASUKA to section 137E is held even for 6th layer to 8th layer. On the other hand, the westward nitrate transport is evident for 2nd layer to 8th layer. Being similar to the eastward nitrate transport, the westward nitrate transport is also intensified from section ASUKA to section 137E.

Because the horizontal variations of nitrate transport are similar among 8 layers, the integration from 1st layer to 8th layer (Fig. 1b) does not show a surprise result to us. The increasing of eastward nitrate transport from the East China Sea to south of Japan as well as the downstream intensification of both eastward and westward nitrate transports from section AUSKA to section 137E is apparent in Fig. 1b.

4 Discussions

4.1 Error caused by using mean nitrite concentration

As we described in Sect. 2, the mean nitrate flux at sections TK and ASUKA are calculated by product of mean current speed and mean nitrate concentration in different period. We now use section 137E as an example to examine the error caused by such treatment.

Figure 6a presents nitrate flux calculated by product of mean current speed for a period of 2000 to 2009 and mean nitrate concentration for the same period of 2000 to 2009. The difference of Fig. 6a and Fig. 4e is presented in Fig. 6b and this difference is the contribution of second term in r.h.s of Eq. (3). The spatial structure of nitrate flux in Fig. 6a is almost the same as that in Fig. 4e. The maximum difference between two mean nitrate fluxes is $\sim 0.8\,\mathrm{mmol\,m^{-2}\,s^{-1}}$(Fig. 6b), being less than 10 % of nitrate flux at the same place shown in Fig. 4e. This result suggests that the contribution of

second term in r.h.s of Eq. (3) to mean nitrate flux is smaller than that of first term in r.h.s of Eq. (3) by one order. Therefore, the approximation using only first term in r.h.s of Eq. (3) at sections TK and ASUKA is likely acceptable.

The second problem in the calculation of mean nitrate flux at sections TK and ASUKA is the different period of data used for current speed and nitrate concentration. This problem is not serious for section ASUKA but is significant for section TK where the period for current speed (2000 to 2009) and that for nitrate concentration (prior 1990) is completely different. This treatment essentially changes the mean nitrate concentration used in first term in r.h.s of Eq. (3). Figure 6c presents nitrate flux calculated by product of mean current speed for the period of 2000 to 2009 and mean nitrate concentration for the period from 1970s to 2011. The difference between Fig. 6c and Fig. 4c is also small (Fig. 6d), suggesting that the influence of using mean nitrate concentration in different period from the current speed does not cause significant change in mean nitrate flux. Therefore, the mean nitrate fluxes for sections TK and ASUKA presented in Figs. 4b and 4c are acceptable as a first approximation to the true values.

4.2 Contribution of Ryukyu Current and Kuroshio recirculation to Kuroshio downstream nitrate transport

For a quantitative estimation on nitrate transport at 5 sections, we present positive volume transport VT^+, positive nutrient transport NT^+, positive transport-averaged nitrate concentration NT^+/VT^+, area-averaged nitrate concentration for the area with positive volume transport C^+, negative volume transport VT^-, negative nutrient transport NT^-, negative transport-averaged nitrate concentration NT^-/VT^-, area-averaged nitrate concentration for the area with negative volume transport C^-, net volume transport $VT = VT^+ + VT^-$, and net nutrient transports $NT = NT^+ + NT^-$ for total and each of 8 isopycnal layers in Table 1.

The section PN and section TK have very similar structure in all terms shown in Table 1. The positive volume transport and nitrate transport is at the same order in all the isopycnal layers at two sections; while the negative volume transport and nitrate

transport are smaller than positive ones by one order. The close value of transports within each of 8 isopycnal layers at two sections suggests that the horizontal nitrate input or vertical nitrate exchange between different isopycnal layers during the Kuroshio path from section PN to section TK is small. In contrast, the reduction of positive vol-
5 ume transport and nitrate transport from section PN to section TK is clear (Table 1). This reduction is consistent with the separation of a branch current from the Kuroshio southwest of Kyushu (Lie et al., 1998; Guo et al., 2006).

The Ryukyu Current plays a more important role in downstream nitrate transport than downstream volume transport. The eastward volume transport is 16.4 Sv at section OK,
10 being smaller than 23.5 Sv at section TK (Table 1). However, the eastward nitrate transport is 341.2 kmol s^{-1} at section OK, being almost two times of that (176.3 kmol s^{-1}) at section TK (Table 1). The same conclusion is also held for net nitrate transport (Table 1). As stated previously, the direct reason for the large nitrate transport at section OK is the deep location of relatively strong current speed where the nitrate concentra-
15 tion is high (Fig. 3).

Another important issue known from values at section OK in Table 1 is the contribution of recirculation. Differing from sections PN and TK, the negative volume and nitrate transports at section OK are at the same order as the positive volume and nitrate transports, respectively. From the distribution of nitrate transport (Fig. 1), we know that the
20 positive nitrate transport is located adjacent to Okinawa Island, corresponding to the Ryukyu Current, while the negative nitrate transport is distributed widely from Okinawa Island to interior region. Therefore, the second reason for the Ryukyu Current to bring more nutrients to the area south of Japan than the Kuroshio in the East China Sea is the contribution of recirculation.
25 The net downstream nitrate transport at section ASUKA is approximately the sum of those at sections TK and OK (Table 1). At section ASUKA, layers 1–5, especially layer 3 (25.50–26.50σ_θ) and layer 4 (26.50–27.00$\sigma_{\theta,}$), are major contribution to the net downstream nitrate transport. Meanwhile, both positive and negative nitrate transports significantly increase at section ASUKA as compared to the sum of them at sections

Full Screen / Esc

Printer-friendly Version

Interactive Discussion

TK and OK, indicating again the contribution of Kuroshio recirculation to the negative nitrate transport as well as positive nitrate transport. As known from Fig. 4, the recirculation-induced negative nitrate transport is large in the subsurface and this point is confirmed again in Table 1 (layers 3–5). As a response to the recirculation-induced negative nitrate transport, the positive nitrate transport in these layers also increases. Consequently, the positive nitrate transport at section ASUKA reaches ∼ 1.8 times of the sum of those at sections TK and OK.

Although sections ASUKA and 137E are very close, the intensification of positive nitrate transport by the recirculation actually develops from section ASUKA to section 137E (Table 1). The net nitrate transport has little difference between two sections, but the positive nitrate transport increases by 50 % from section ASUKA to section 137E. Considering the distance from section ASUKA to section 137E and that from section TK or section OK to section ASUKA, the increasing rate of positive nitrate transport along the Kuroshio path is larger in former region than in latter region. Therefore, it is likely that the intensification of positive nitrate transport by the recirculation is not spatially uniform along the Kuroshio path.

It must be noted that the negative nitrate transport is larger at section 137E than at section ASUKA. This means that a part of negative nitrate transport return to the Kuroshio path in the area between two sections. Therefore, a clear image can be drawn for the contribution of Kuroshio recirculation that merger into the Kuroshio main stream and increase the positive nitrate transport along the Kuroshio.

As described above, the recirculation-induced increasing of downstream volume transport of the Kuroshio is apparent and can be considered as the primary cause for the downstream intensification of nitrate transport along the Kuroshio. A second candidate responsible for the intensification of nitrate transport along the Kuroshio is the downstream change of nitrate concentration in the water carried by the Kuroshio. As shown in Table 1, the positive transport-averaged nitrate concentration and area-averaged nitrate concentration for area with positive volume transport generally decrease from section PN to section TK in all the layers; generally increase from section

TK or section OK to section ASUKA in all the layers except for layers 4–6; and generally increase from section ASUKA to section 137E in all the layers except for layer 1 and layers 7–8.

Williams et al. (2011) reported the same downstream strengthening of nutrient transport occurs along the Gulf Stream and concluded that the primary cause for the increasing in nutrient transport is the recirculation-induced increasing of downstream volume transport of Gulf Stream while the second cause is the downstream increasing of nutrient concentration in the water carried by the Gulf Stream in denser layers. In addition, they reported a downstream decreasing of nutrient concentration in the water carried by the Gulf Stream in light layers and confirmed that the lateral water exchange in the same isopycnal layer in the cause for downstream increasing and decreasing of nutrient concentration in the water carried by the Gulf Stream. Although all these processes likely occur in the Kuroshio, they are not easily applied to the Kuroshio region without any modification because the downstream variations in nitrate concentration in the Kuroshio region cannot be summarized only by the reduction in light layers and raising in dense layers.

5 Summary

Using repeated hydrographic data from 2000 to 2009 and an inverse method, we obtained absolute geostrophic current speed at 4 sections along the Kuroshio from the East China Sea (sections PN and TK) to south of Japan (sections ASUKA and 137E) and at a section southeast of Ryukyu Islands (section OK). The vertical structures and volume transports of temporally averaged velocity at these sections are generally consistent with previous understanding on the Kuroshio and Ryukyu Current there. In addition, the presence of Kuroshio recirculation is confirmed at sections OK, ASUKA and 137E.

Using absolute geostrophic current speed and nitrate concentration measured at 5 sections, we then obtained nitrate fluxes and their temporal mean. The presence of

subsurface maximum core in nutrient flux, as reposted in Gulf Stream (Pelegrí and Csanady, 1991; Pelegrí et al., 1996) and at section PN (Guo et al., 2012), is confirmed at all the sections and their depths are 400, 500, 500, 400, and 800 m for sections PN, TK, ASUKA, 137E and OK, respectively, indicating a stable nutrient stream along the Kuroshio from the East China Sea to south of Japan. The eastward nitrate transport carried by this stable nutrient stream is 199.3, 176.3, 341.2, 909.2, and 1385.5 kmol s^{-1} for sections PN, TK, OK, ASUKA, and 137E, respectively.

The deeper subsurface maximum core of nitrate flux at section OK than at the other sections is induced by the vertical structure of Ryukyu Current, which has a subsurface maximum current speed (Zhu et al., 2004). This in turn results a larger nitrate transport at section OK than at section TK, suggesting that the Ryukyu Current brings more nutrients than the Kuroshio in the East China Sea to the region south of Japan.

The other reason for the larger nitrate transport at section OK than at section TK is the contribution of recirculation whose nitrate transport is small at section TK but large at section OK. The role of recirculation is more evident at sections ASUKA and 137E, between which the recirculation increases the eastward nitrate transport by a factor of 1.5. In fact, the eastward nitrate transport at ASUKA is larger than the sum of those at sections TK and OK by a factor of 1.8, again suggesting the significant role of recirculation in increasing Kuroshio eastward nitrate transport.

The downstream intensification of nutrient transport is a common feature in the Gulf Stream nutrient stream and Kuroshio nutrient stream. The recirculation and its contribution to the nutrient transport occur in both streams. A special feature in the northwest Pacific is the effect of Ryukyu Current that has a deep strong current and transports more nutrient than the Kuroshio in the East China Sea to the Kuroshio south of Japan. Another difference between the Gulf Stream and Kuroshio is the downstream variation of nutrient concentration in the water carried by two western boundary currents. The nitrate concentration decreases in the light layer but increase in dense layer along with the Gulf Stream. However, the downstream variation in the Kuroshio region is not as

Kuroshio nutrient transport from the East China Sea to south of Japan

X. Y. Guo et al.

⏮ | ⏭

◀ | ▶

Back | Close

Full Screen / Esc

Printer-friendly Version

Interactive Discussion

simple as that in the Gulf Stream. Therefore, more complex processes are expected in the Kuroshio region and must be investigated in the future.

References

Andres, M., Park, J.-H., Wimbush, M., Zhu, X.-H., Chang, K.-I., and Ichikawa, H.: Study of the Kuroshio/Ryukyu Current system based on satellite-altimeter and in situ data measurements, J. Oceanogr., 64, 937–950, 2008.

Aoyama, M., Goto, H., Kamiya, H., Kaneko, I., Kawae, S., Kodama, H., Konishi, Y., Kusumoto, K., Miura, H., Moriyama, E., Murakami, K., Nakano, T., Nozaki, F., Sasano, D., Shimizu, T., Suzuki, H., Takatsuki, Y., and Toriyama, A.: Marine biogeochemical response to a rapid warming in the main stream of the Kuroshio in the western North Pacific, Fish. Oceanogr., 17, 206–218, 2008.

Chen, C. T. A., Liu, C. T., and Pai, S. C.: Transport of oxygen, nutrients and carbonates by the Kuroshio Current, Chin. J. Oceanol. Limn., 12, 220–227, 1994.

Chen, C. T. A., Liu, C. T., and Pai, S. C.: Variations in oxygen, nutrient and carbonate fluxes of the Kuroshio Current, La mer, 33, 161–176, 1995.

Guo, X., Miyazawa, Y., and Yamagata, T.: The Kuroshio onshore intrusion along the shelf break of the East China Sea: the origin of the Tsushima warm current, J. Phys. Oceanogr., 36, 2205–2231, 2006.

Guo, X., Zhu, X.-H., Wu, Q.-S., and Huang, D.: The Kuroshio nutrient stream and its temporal variation in the East China Sea, J. Geophys. Res., 117, C01026, doi:10.1029/2011JC007292, 2012.

Hasunuma, K. and Yoshida, K.: Splitting of the subtropical gyre in the Western North Pacific, J. Oceanogr. Soc. Jpn., 34, 160–172, 1978.

Ichikawa, H., Nakamura, H., Nishina, A., and Higashi, M.: Variability of north-eastward current southeast of northern Ryukyu Islands, J. Oceanogr., 60, 351–363, 2004.

Imawaki, S., Hiroshi, U., Ichikawa, H., Fukazawa, M., and Umatani, S., and ASUKA Group: satellite altimeter monitoring the Kuroshio transport south of Japan, Geophys. Res. Lett., 28, 17–20, 2001.

Lie, H.-J., Cho, C.-H., Lee, J.-H., Niiler, P., and Hu, J.-H.: : Separation of the Kuroshio water and its penetration onto the continental shelf west of Kyushu, J. Geophys. Res., 103, 2963–2976, 1998.

Pelegrí, J. L. and Csanady, G. T.: Nutrient transport and mixing in the Gulf Stream, J. Geophys. Res., 96, 2577–2583, 1991.

Pelegrí, J. L., Csanady, G. T., and Martins, A.: The North Atlantic nutrient stream, J. Oceanogr., 52, 275–299, 1996.

Williams, R. G., McDonagh, E., Roussenov, V. M., Torres Valdes, S., King, B., Sanders, R., and Hansell, D. A.: Nutrient streams in the North Atlantic: advective pathways of inorganic and dissolved organic nutrients, Global Biogeochem. Cy., 25, GB4008, doi:10.1029/2010GB003853, 2011.

Wunsch, C.: The North Atlantic general circulation west of 50° W determined by inverse methods, Rev. Geophys. Space Phys., 16, 583–620, 1978.

Zhu, X.-H., Ichikawa, H., Ichikawa, K., and Takeuchi, K.: Volume transport variability southeast of Okinawa Island estimated from satellite altimeter data, J. Oceanogr., 60, 953–962, 2004.

Zhu, X.-H., Park, J.-H., and Kaneko, I.: Velocity structures and transports of the Kuroshio and the Ryukyu Current during fall of 2000 estimated by an inverse technique, J. Oceanogr., 62, 587–596, 2006.

Table 1. Positive volume transport VT^+, positive nutrient transport NT^+, positive transport-averaged nitrate concentration NT^+/VT^+, area-averaged nitrate concentration for area with positive volume transport C^+, negative volume transport VT^-, negative nutrient transport NT^-, negative transport-averaged nitrate concentration NT^-/VT^-, area-averaged nitrate concentration for area with negative volume transport C^-, net volume transport $VT = VT^+ + VT^-$, net nutrient transports $NT = NT^+ + NT^-$ for total and each of 8 isopycnal layers. The line with the name of section has value for total 8 isopycnal layers. "NaN" means no data.

	VT^+ (Sv)	NT^+ (kmol s^{-1})	NT^+/VT^+ (mmol m^{-3})	C^+ (mmol m^{-3})	VT^- (Sv)	NT^- (kmol s^{-1})	NT^-/VT^- (mmol m^{-3})	C^- (mmol m^{-3})	VT (Sv)	NT (kmol s^{-1})
PN	**26.2**	**199.3**	**7.6**	**18.3**	**−2.8**	**−28.6**	**10.2**	**18.0**	**23.4**	**170.7**
Layer 1	13.9	23.5	1.7	1.9	−1.3	−1.3	1.0	1.4	12.6	22.3
Layer 2	4.7	34.0	7.2	7.1	−0.5	−3.0	6.1	6.3	4.2	31.0
Layer 3	5.8	88.5	15.2	16.2	−0.5	−8.4	15.4	16.5	5.3	80.1
Layer 4	1.4	41.4	28.6	29.8	−0.3	−9.9	29.6	29.5	1.1	31.5
Layer 5	0.3	11.9	36.1	36.4	−0.2	−6.1	36.3	36.4	0.2	5.8
TK	**22.9**	**176.3**	**7.7**	**17.2**	**−0.8**	**−9.1**	**12.0**	**20.2**	**22.2**	**167.3**
Layer 1	11.3	15.0	1.3	1.3	−0.5	−0.3	0.5	0.7	10.8	14.8
Layer 2	4.4	29.6	6.7	6.7	0.0	−0.1	5.2	4.9	4.4	29.5
Layer 3	5.4	78.8	14.7	14.5	NaN	NaN	NaN	NaN	5.4	78.8
Layer 4	1.5	42.3	27.6	28.1	NaN	NaN	NaN	NaN	1.5	42.3
Layer 5	0.3	10.6	34.4	35.1	0.0	−1.0	35.8	35.9	0.3	9.6
Layer 6	NaN	NaN	NaN	NaN	−0.2	−7.7	39.1	39.1	−0.2	−7.7
OK	**16.3**	**341.2**	**21.0**	**26.6**	**−10.6**	**−189.4**	**17.8**	**26.5**	**5.6**	**151.9**
Layer 1	2.5	2.6	1.0	0.9	−2.8	−1.9	0.7	0.8	−0.3	0.7
Layer 2	2.6	14.8	5.7	5.7	−1.9	−10.8	5.6	5.7	0.7	4.1
Layer 3	3.9	61.3	15.7	16.5	−2.1	−32.6	15.7	16.4	1.8	28.7
Layer 4	2.5	76.7	31.0	32.0	−1.1	−32.8	31.2	31.5	1.4	43.9
Layer 5	2.0	75.2	38.3	39.0	−0.8	−31.0	38.6	38.8	1.2	44.2
Layer 6	1.4	56.7	40.2	40.4	−0.9	−38.1	40.4	40.4	0.5	18.6
Layer 7	0.7	29.7	39.7	39.7	−0.6	−22.3	39.8	39.8	0.2	7.4
Layer 8	0.6	24.0	38.9	38.8	−0.5	−19.9	38.7	38.8	0.1	4.2
ASUKA	**61.8**	**909.2**	**14.7**	**27.2**	**−35.0**	**−549.8**	**15.7**	**26.8**	**26.8**	**359.4**
Layer 1	17.1	48.8	2.8	2.2	−6.9	−5.1	0.7	0.6	10.2	43.7
Layer 2	14.2	95.8	6.8	5.9	−9.4	−46.0	4.9	5.0	4.7	49.7
Layer 3	16.0	254.4	15.9	16.9	−8.5	−130.6	15.3	16.1	7.4	123.8
Layer 4	6.9	206.3	29.8	31.3	−3.8	−114.2	30.4	31.1	3.2	92.1
Layer 5	3.3	126.6	38.4	39.1	−2.4	−93.2	38.5	39.0	0.9	33.3
Layer 6	2.0	83.3	41.0	41.4	−1.8	−73.9	41.3	41.4	0.2	9.4
Layer 7	1.2	48.9	41.0	41.0	−1.1	−45.6	41.0	41.0	0.1	3.3
Layer 8	1.1	45.2	40.1	40.2	−1.0	−41.1	40.0	40.1	0.1	4.1
137E	**75.3**	**1385.5**	**18.4**	**27.4**	**−51.5**	**−1040.3**	**20.2**	**26.7**	**23.8**	**345.2**
Layer 1	16.0	39.7	2.5	2.1	−8.0	−6.6	0.8	0.7	8.0	33.1
Layer 2	15.4	128.4	8.3	7.7	−10.9	−54.9	5.0	5.0	4.5	73.5
Layer 3	20.4	372.2	18.2	18.5	−10.9	−167.9	15.3	15.8	9.5	204.3
Layer 4	9.0	271.1	30.3	30.8	−6.0	−180.3	30.2	30.6	3.0	90.8
Layer 5	5.4	203.4	37.8	38.2	−4.7	−182.5	38.8	39.0	0.7	20.9
Layer 6	4.5	184.8	41.0	41.0	−5.0	−204.7	41.3	41.4	−0.4	−19.9
Layer 7	2.8	114.6	40.7	40.7	−3.5	−142.5	41.0	41.0	−0.7	−27.9
Layer 8	1.8	71.2	39.8	39.9	−2.5	−100.9	40.1	40.1	−0.7	−29.7
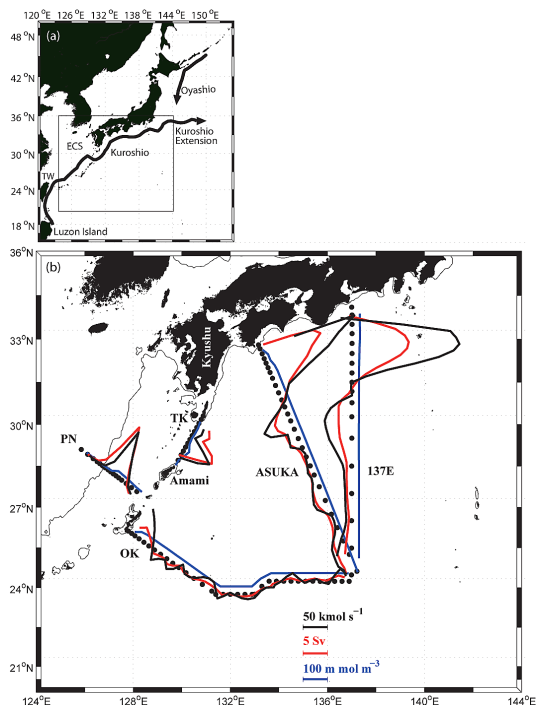
Fig. 1. (a) Study area and schematic image of Kuroshio path. "ECS" denotes East China Sea; "TW" denotes Taiwan. **(b)** Position of hydrographic stations (black dots), nitrate concentration (blue line, $\mathrm{mmol\,m^{-3}}$) averaged from sea surface to deepest layer within 25 km width, volume transport (red line, $\mathrm{Sv} = 10^6\,\mathrm{m^3\,s^{-1}}$) and nitrate transport (black line, $\mathrm{kmol\,s^{-1}}$) integrated from sea surface to deepest layer within 25 km width. See Eqs. (4–6) and their description in Sect. 2 for the calculation method of these variables. "PN", "TK", "OK", "ASUKA", and "137E" are the name of sections. The thin line denotes 200 m isobath.
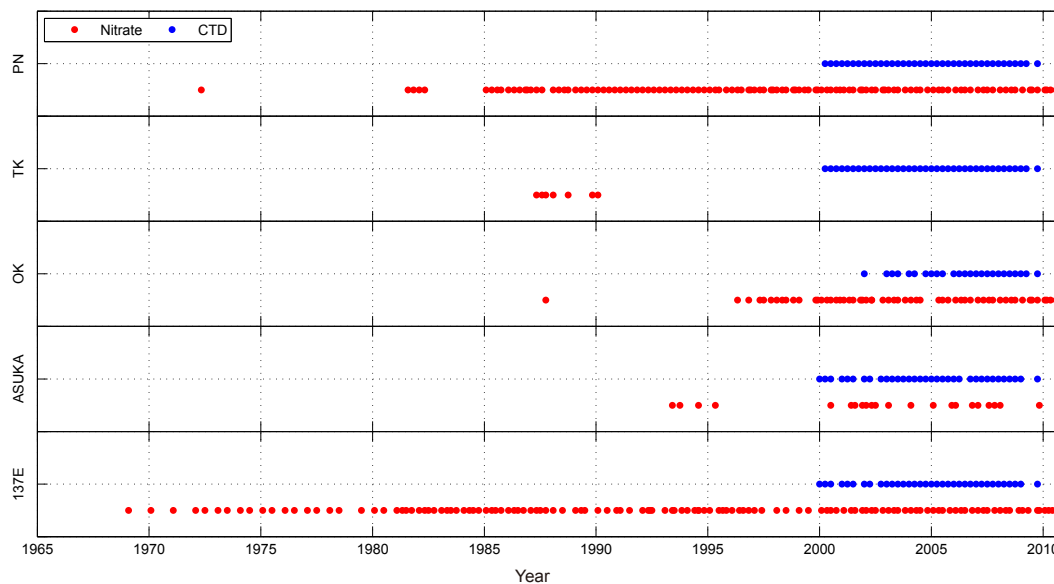
Fig. 2. Data distribution at five sections. Blue dots denote the time when hydrographic data collected by CTD were available; red dots denote the time when nitrate concentration were reported.
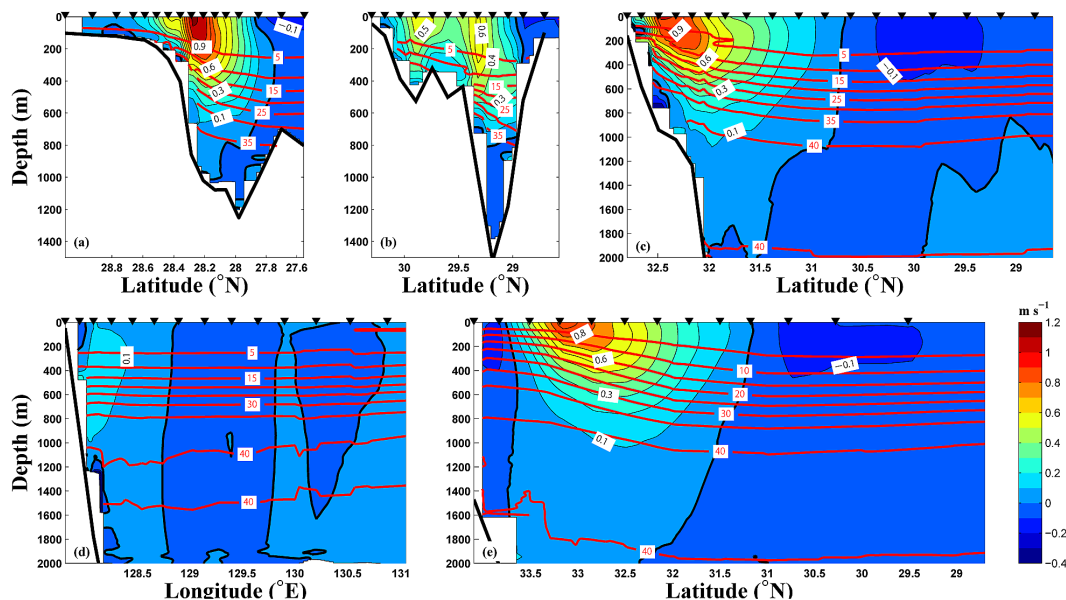
Fig. 3. Temporally averaged absolute geostrophic velocity ($m\,s^{-1}$) and nitrate concentration ($mmol\,m^{-3}$) at the sections. Color tone and black contour lines show velocity with an interval of $0.1\,m\,s^{-1}$. Positive values indicate eastward velocity. Red contour lines indicate nitrate concentration with an interval of $5\,mmol\,m^{-3}$. Thick black line shows zero speed. The inverse triangles denote hydrographic stations where water temperature, salinity, and nitrate concentration are available.

Fig. 4. Temporally averaged nitrate flux ($\mathrm{mmol\,m^{-2}\,s^{-1}}$) at the sections. Color tone and black contour lines show nitrate flux with an interval of $1\,\mathrm{mmol\,m^{-2}\,s^{-1}}$. Positive values indicate eastward flux. Red contour lines indicate 8 isopycnal layers in the inverse calculation. Thick black line shows zero nitrate flux. The inverse triangles are the same as those in Fig. 3.
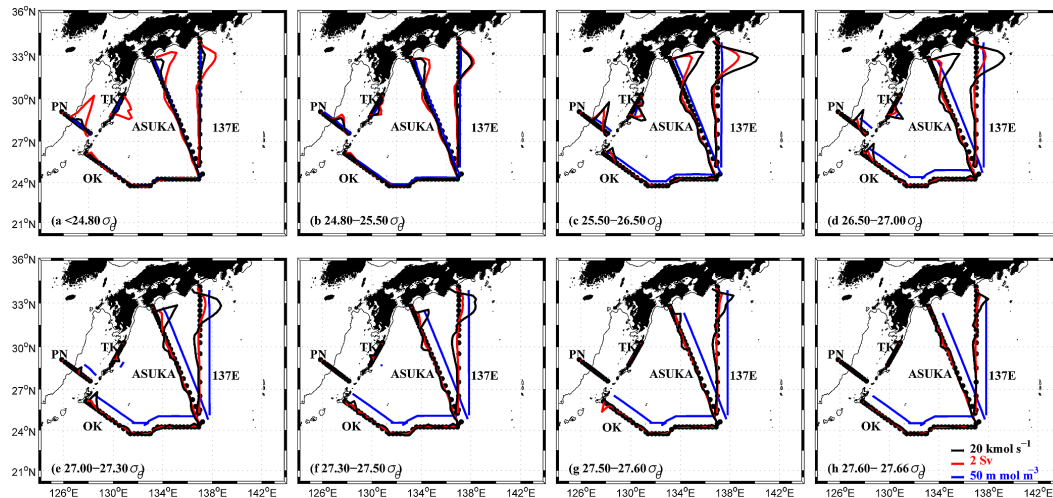
Fig. 5. The same as Fig. 1b but for each of 8 isopycnal layers: **(a)** sea surface–24.8σ_θ, **(b)** 24.8–25.5σ_θ, **(c)** 25.5–26.5σ_θ, **(d)** 26.5–27σ_θ, **(e)** 27–27.3σ_θ, **(f)** 27.3–27.5σ_θ, **(g)** 27.5–27.6σ_θ, **(h)** 27.6–27.66σ_θ.
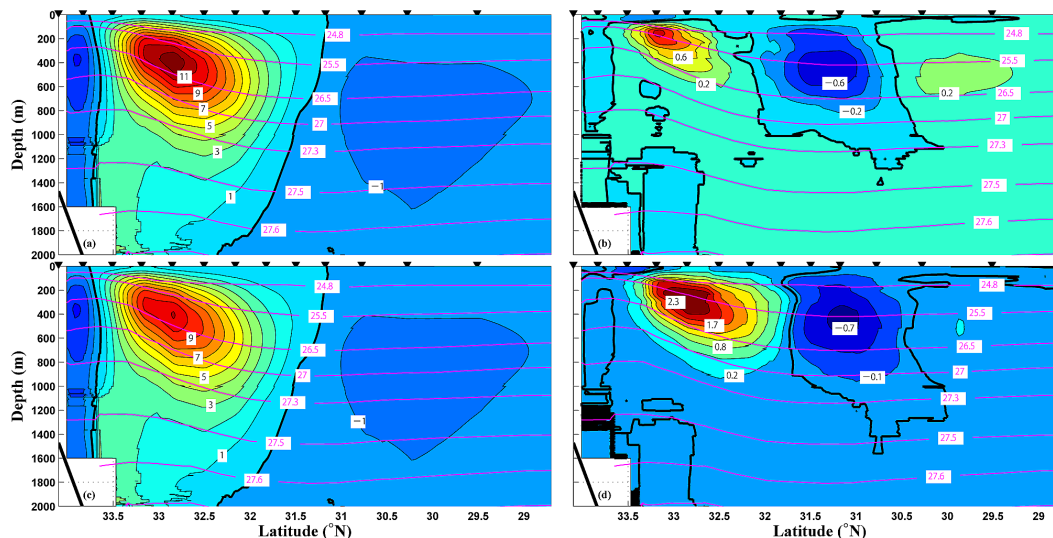
Fig. 6. Nitrate flux (mmol m^{-2} s^{-1}) at section 137E calculated by temporally averaged speed and temporally averaged nitrate concentration **(a)** for all the period shown in Fig. 2; **(b)** difference between Fig. 3e and **(a)**; **(c)** for the period from 2000 to 2009; **(d)** difference between Fig. 3e and **(c)**. Color tone and black contour lines show nitrate flux with an interval of 1 mol m^{-2} s^{-1} in **(a)** and **(c)**, with an interval of 0.2 mol m^{-2} s^{-1} in **(b)**, and with an interval of 0.3 mol m^{-2} s^{-1} in **(d)**. Positive values indicate eastward flux. Red contour lines indicate 8 isopycnal layers. Thick black line shows zero nitrate flux. The inverse triangles denote hydrographic stations where water temperature, salinity, and nitrate concentration are available.

Title Page

Abstract | Introduction

Conclusions | References

Tables | Figures

◄◄ | ►►

◄ | ►

Back | Close

Full Screen / Esc

Printer-friendly Version

Interactive Discussion